The State Scientific Center of Russia
The Budker Institute of Nuclear Physics
SB RAS

V.N. Baier, V.M. Katkov
and V.M. Strakhovenko

ELECTRON-PHOTON CASCADE IN ORIENTED CRYSTALS AT HIGH ENERGIES

Budker INP 95-85

НОВОСИБИРСК

Electron-photon Cascade in Oriented Crystals at High Energies

V. N. Baier, V. M. Katkov and V. M. Strakhovenko

Budker Institute of Nuclear Physics,
630090 Novosibirsk, Russia

Abstract

The development of an electromagnetic cascade in axially aligned single crystal is discussed for energy of initial electrons and photons from tens to hundreds GeV. The method of successive approximations for solution of a set of kinetic equations is analyzed. Numerical calculations are performed to obtain energy and thickness dependence of cascade characteristics. The results are in a good agreement with available experimental data.

1 Introduction

It is well known that the mechanisms of photon emission [1] and pair production [2] processes in single crystals depend on the angle of incidence of an initial particle ϑ_0 with respect to crystal axes or planes. At sufficiently high particle energy these coherent effects appear to be especially strong for $\vartheta_0 \ll V_0/m$ (V_0 is the scale of corresponding potential) at axial alignment, being one to two order of magnitude larger than in corresponding amorphous medium. Along with spectra of created particles and photons are also very different from those providing by Bethe-Heitler (BH) mechanism, it naturally leads to many distinctive features (see [3]) of the specific electron-photon cascade in oriented single crystal as compared to that in amorphous medium.

Let us remind that the pair production probability in the field of crystal axes falls off exponentially for photon energy below ω_t, revealing some kind of threshold behavior. We determine ω_t more definitely as follows

$$W_e(\omega_t) = W_e^{BH}, \tag{1}$$

where W_e^{BH} is the pair production probability in corresponding amorphous medium. When initial particle energy ε_0 (ω_0) $\gg \omega_t$ and lower boundary of recorded particle energy $\varepsilon_f \geq \omega_t$, coherent mechanism dominate in both pair production and photon emission processes during cascade development. We call it *hard cascade*, which properties were investigated in [3], where under some simplifying assumptions analytical solutions of kinetic equations (2) in

the next section were obtained. When $\varepsilon_0 < \omega_t$ and $\varepsilon_f \ll \omega_t$ (we call it *soft cascade*) the pair production occurs owing to BH mechanism, while photon emission is still dominated by the coherent one. Some properties of a *soft cascade* were investigated in [4], where, in particular, a model spectrum of radiation at axial alignment was suggested used in the present paper too. And, finally, we call *mixed cascade* the situation when ε_0 $(\omega_0) > \omega_t$ (or ε_0 $(\omega_0) \gg \omega_t$), while $\varepsilon_f \ll \omega_t$ and both coherent and BH mechanisms contribute at different stages of the cascade development.

In the present paper mainly dedicated to investigation of the *mixed cascade*, we first obtain an formal solution of kinetic equations (2) as an infinite sum of terms corresponding to increasing number of created generations of charged particles taken into account and discuss a region of the applicability of first approximation in this expansion. Then we perform numerical calculations (Monte-Carlo simulation) for < 110 > axis of Ge single crystal and obtain dependence of cascade characteristics on initial particle type, crystal thickness (up to 5 cm), and initial particle energy in the range from a few tens to a few hundreds of GeV.

The development of an electron-photon cascade at axial alignment has been observed and investigated for the first time in [5]. We have compared our results to those of [5] and have found a quite good agreement with experimental data.

2 The method of successive approximations

Assuming that the probabilities of the emission of radiation from electrons and positrons are the same [1],the electromagnetic shower development is described by the following set of integro-differential equations [6]

$$\begin{aligned}
\frac{\partial N_\gamma(\omega,t)}{\partial t} &= -W_e(\omega)N_\gamma(\omega,t) + \int_\omega^\infty d\varepsilon W_\gamma(\varepsilon,\omega)N_e(\varepsilon,t), \\
\frac{\partial N_e(\varepsilon,t)}{\partial t} &= -W_\gamma(\varepsilon)N_e(\varepsilon,t) + \int_\varepsilon^\infty d\varepsilon' W_\gamma(\varepsilon',\varepsilon'-\varepsilon)N_e(\varepsilon',t) \\
&\quad +2\int_\varepsilon^\infty d\omega W_e(\omega,\varepsilon)N_\gamma(\omega,t),
\end{aligned} \tag{2}$$

[1] It is well known that in a thin crystal as a consequence of a flux redistribution determined by initial conditions electrons may radiate more strongly than positrons. However, the full-scale cascade can develop only in thick crystals where the distribution of both electrons and positrons in the transverse phase space becomes uniform, resulting in the same radiation.

where $N_\gamma(\omega,t)$ and $N_e(\varepsilon,t)$ are energy distribution functions of photons and electrons over correspondingly ω and ε at a given depth t; $W_\gamma(\varepsilon,\omega)$ is the spectral probability of the emission of a photon with the energy ω from a charged particle with the energy ε and $W_e(\omega,\varepsilon)$ is the probability of electron-positron pair production by a photon with the energy ω differential over the energy ε of one of the created particles while that of the other is $\omega-\varepsilon$; $W_\gamma(\varepsilon) = \int_0^\varepsilon d\omega W_\gamma(\varepsilon,\omega)$ is the total probability of radiation and $W_e(\omega)$ is the total probability of pair production by a photon with energy ω.

The set of equations (2) can be rewritten as:

$$\begin{aligned}
N_\gamma(\omega,t) &= N_\gamma(\omega,0)e^{-W_e(\omega)t} + \int_0^t d\tau e^{-W_e(\omega)(t-\tau)} \int_\omega^\infty d\varepsilon W_\gamma(\varepsilon,\omega)N_e(\varepsilon,\tau), \\
N_e(\varepsilon,t) &= N_e^{(0)}(\varepsilon,t) + 2\int_0^t d\tau \int_\varepsilon^\infty d\varepsilon' \int_{\varepsilon'}^\infty d\omega W_e(\omega,\varepsilon')N_\gamma(\omega,t-\tau)N_0(\varepsilon';\varepsilon,\tau),
\end{aligned} \tag{3}$$

where as in [3] the function $N_0(\varepsilon';\varepsilon,t)$ appears describing the evolution along the depth t of the energy distribution of initially (at $t=0$)monochromatic charged particles ($N_0(\varepsilon';\varepsilon,0) = \delta(\varepsilon'-\varepsilon)$) due to photon emission only:

$$\frac{\partial N_0(\varepsilon';\varepsilon,t)}{\partial t} = -W_\gamma(\varepsilon)N_0(\varepsilon';\varepsilon,t) + \int_\varepsilon^\infty d\varepsilon'' W_\gamma(\varepsilon'',\varepsilon''-\varepsilon)N_0(\varepsilon';\varepsilon'',t). \tag{4}$$

The functions $N_\gamma(\omega,0)$ and $N_e^{(0)}(\varepsilon,t)$ are defined by the initial conditions. If the initial particle is a photon with the energy ω_0 then $N_e^{(0)}(\varepsilon,t) = 0$, $N_\gamma(\omega,0) = \delta(\omega-\omega_0)$; and for the initial charged particle with the energy ε_0 we have $N_\gamma(\omega,0) = 0$ and $N_e^{(0)}(\varepsilon,t) = N_0(\varepsilon_0;\varepsilon,t)$.

Let us consider now the case when the initial particle is an electron with the energy ε_0 .Using eq.(3),we have

$$\begin{aligned}
N_e(\varepsilon,t) &= N_0(\varepsilon_0;\varepsilon,t) + 2\int_0^t d\tau \int_0^{t-\tau} d\tau' \int_\varepsilon^\infty d\varepsilon' \int_{\varepsilon'}^\infty d\omega \int_\omega^\infty d\varepsilon'' N_e(\varepsilon'',\tau') \\
&\times W_\gamma(\varepsilon'',\omega)W_e(\omega,\varepsilon')N_0(\varepsilon';\varepsilon,\tau)e^{-W_e(\omega)(t-\tau-\tau')}.
\end{aligned} \tag{5}$$

Performing in eq.(5) the Laplace transform over t:

$$N_e(\varepsilon,p)=\int\limits_0^\infty N_e(\varepsilon,t)e^{-pt}dt\ ,\quad etc..$$

we obtain

$$N_e(\varepsilon,p)=N_0(\varepsilon_0;\varepsilon,p)+\int\limits_\varepsilon^\infty d\varepsilon' N_e(\varepsilon',p)R(\varepsilon',\varepsilon,p), \tag{6}$$

where

$$R(\varepsilon',\varepsilon,p)=2\int\limits_0^{\varepsilon'}d\omega\int\limits_0^{\omega}d\varepsilon''\frac{W_\gamma(\varepsilon',\omega)W_e(\omega,\varepsilon'')N_0(\varepsilon'';\varepsilon,p)}{p+W_e(\omega)}. \tag{7}$$

The kernel $R(\varepsilon',\varepsilon,p)$ describes emission of a photon with the energy ω from a charged particle with the energy ε'; then conversion of this photon into a pair of charged particles one of which has the energy ε'' and subsequent development of energy distribution owing to photons emission from this particle.

The solution of eq.(6)can be represented in the following form:

$$N_e(\varepsilon,p)=\int\limits_\varepsilon^\infty d\varepsilon_1 N_0(\varepsilon_0;\varepsilon_1,p)S(\varepsilon_1,\varepsilon,p), \tag{8}$$

where

$$S(\varepsilon_1,\varepsilon,p)=\delta(\varepsilon_1-\varepsilon)+R(\varepsilon_1,\varepsilon,p)+\int d\varepsilon_2 R(\varepsilon_1,\varepsilon_2,p)R(\varepsilon_2,\varepsilon,p)$$
$$+\int d\varepsilon_2 d\varepsilon_3 R(\varepsilon_1,\varepsilon_2,p)R(\varepsilon_2,\varepsilon_3,p)R(\varepsilon_3,\varepsilon,p)+.. \tag{9}$$

with the evident structure of this infinite series. The first term of the series (9) allows for the evolution of the initial distribution due to photons emission only (zero approximation). The second one (first approximation) takes into account creation of charged particles of the first generation by emitted photons etc.

The inverse Laplace transform of eq.(8) in accordance with the expansion (9) gives a decomposition for $N_e(\varepsilon,t)$:

$$N_e(\varepsilon,t)=\sum_{n=0}^{\infty}N_e^{(n)}(\varepsilon,t).$$

The function $N_e^{(n)}(\varepsilon,t)$ contains $2n$-fold integral over depth and $3n$-fold integral over energies of charged particles and photons. For example, the first approximation reads

$$N_e^{(1)}(\varepsilon,t)=\ 2\int\limits_0^t d\tau\int\limits_0^{t-\tau}d\tau'\int\limits_\varepsilon^\infty d\varepsilon_2\int\limits_{\varepsilon_2}^\infty d\omega\int\limits_\omega^\infty d\varepsilon_1 N_0(\varepsilon_0;\varepsilon_1,\tau)$$
$$\times\ \exp[-W_e(\omega)(t-\tau-\tau')]W_\gamma(\varepsilon_1,\omega)W_e(\omega,\varepsilon_2)N_0(\varepsilon_2;\varepsilon,\tau'). \tag{10}$$

For sufficiently small depth the function $N_e^{(1)}(\varepsilon,t)$ can be used as a distribution function of created charged particles, but with increasing depth such description becomes at long last invalid. For quantitative analysis of the problem we have compared the total number of created charged particles with energy $\varepsilon>\varepsilon_f$ to the quantity

$$N_e^{(1)}(t)=\int\limits_{\varepsilon_f}^{\varepsilon_0}N_e^{(1)}(\varepsilon,t)d\varepsilon$$

for different depths in the simplest (for numerical calculations) case of an amorphous medium. For the function $N_0(\varepsilon_0;\varepsilon,\tau)$ the same approximation as in [3] was used :

$$N_0(\varepsilon_0;\varepsilon,\tau)=\delta(\varepsilon-\varepsilon_0\exp(-\tau/L_{rad})).$$

We have found that qualitatively the dependence of the function $N_e^{(1)}(t)$ on depth is the same as for exact solution: it increases until

$$t=t_{op}\simeq L_{rad}\ln\frac{\varepsilon_0}{\varepsilon_f},$$

where it attains the maximum and then drops exponentially. However, the first approximation becomes invalid at a depth much smaller than t_{op}. More definitely, in our example for $\varepsilon_f=5\ MeV$ and ε_0 from 50 GeV to 300 GeV

for $t = 0.45 L_{rad}$ the value of $N_e^{(1)}(t)$ is smaller than exact result by 5-7 % and the difference increases with a further increase of t. A rough estimation of the ratio $N_e^{(2)}/N_e^{(1)}$ for sufficiently small depth, which characterize an accuracy of the first approximation reads

$$\frac{N_e^{(2)}}{N_e^{(1)}} \sim \frac{1}{12} W_\gamma W_e t^2. \qquad (11)$$

It follows from this estimate that the accuracy of the first approximation is better than 10 % for $t < \frac{L_{rad}}{\sqrt{\ln \varepsilon_0/\varepsilon_f}}$. So, generally speaking, for the validity of the first approximation of presented perturbation theory "over a number of generations", we need only weak inequality $t < L_{rad}$ to be satisfied while estimates made in [3] are valid only if $t \ll L_{rad}$.

To obtain corresponding estimates for the crystal case, one should substitute into eq.(11) the probabilities $W_\gamma(\varepsilon_0)$ and $W_e(\omega_c(\varepsilon_0))$ where ω_c is a characteristic energy of photons emitted in an oriented crystal from a charged particle with the energy ε_0. Let us note that when $\varepsilon_0 \leq \omega_t$ (soft cascade) the expression for the optimal thickness t_{op} in crystals is the same as in amorphous medium (see [3], [4]). For $\varepsilon_0 \gg \omega_t$ (mixed cascade), we have

$$t = t_{op} \simeq L_{rad} \ln \frac{\omega_t}{\varepsilon_f},$$

All these estimates have been maid for $\varepsilon_f \ll \omega_t$ with ω_t defined in (1).

3 Numerical calculations and results analysis

Using Monte-Carlo simulation,we have studied electromagnetic shower properties in Ge single crystal for particles incident along $< 110 >$ axis with energies from a few tens to a few hundreds of GeV . The incoherent contributions to probabilities $W_\gamma(\varepsilon, \omega)$ and $W_e(\omega, \varepsilon)$; ionizations energy losses and multiple scattering were described by formulae given in [4]. The coherent contribution to the photon emission probability was calculated according to eq.(2) of [4] giving model description of radiation spectrum at axial channeling. For high energies it turns into intensity spectrum calculated in constant field approximation (CFA). The coherent contribution to the electron-positron pair production probability was calculated in CFA also.

All the results obtained describe the charged particles (photons) created within a crystal (the initial particle was not recorded) and going out from a

crystal. Initial particles momenta were assumed to be aligned exactly along the axis chosen. Usually particles with energies satisfying the inequality $\varepsilon > \varepsilon_f = 5\ MeV$ were recorded.

The total number of charged particles with $\varepsilon > 5\ MeV$ is shown in Fig.1 vs crystal thickness $t = L$. Fig.1(a) is for initial electrons with energies indicated. Fig.1(b) is the same but for particles having outgoing angles with respect to the momentum of the initial electron satisfying the condition $\vartheta_{out} < 0.1$ what corresponds along with energies chosen to the experimental conditions of [5]. The experimental results of [5] are also presented in Fig.1(b). It is seen that theory and experiment are in a good agreement . Fig.1(c) is for initial photons.Comparing Fig.1(a) to Fig.1(c), one can see that the curves presenting numbers of created charged particles are quite similar in shape for the given initial energy and with increasing energy the quantitative difference between them is decreasing, so that a dependence on a type of the initial particle becomes weaker at higher initial energies. It is clear that for the crystal type under consideration ($L_{rad} = 2.3$cm) the optimal thickness is larger than 5 cm. However, if there are additional restrictions on the phase space of created particles (like $\vartheta_{out} < 0.1$ above) the optimal thickness decreases. Corresponding curves become more smooth what is especially visible for $\varepsilon_0 = 40\ GeV$ in Fig.1(b).

In Fig.2 the number of created charged particles vs the energy of the initial particle (an electron or a photon) is given for crystal thickness $L = 2.5\ cm$. The monotonous increase of the yield and mentioned closing in of the curves is seen when energy increases.

The angular distribution of the created charged particles is presented in Fig.3. The harder are the particles the narrower is the angular distribution. This is evident though from the very beginning since multiple scattering becomes less effective and natural angular spread inherent to QED-processes $\sim m/\varepsilon$ is narrowing with the increase of energy. We have found also that when the initial energy increases (calculations were performed also for $\varepsilon_0 = 150\ GeV$ and $\varepsilon_0 = 300\ GeV$) the angular distribution narrows comparing to that shown in Fig.3 but this narrowing is less pronounced for larger boundary energy ε_f.

The spectral distributions of charged particles and photons are shown in Fig.4(a) and (b) respectively for different energies of incident electrons and various crystal thicknesses. The most of the particles are created with relatively low energy and continue to lose it as far as moving within a crystal. The emitted photons will be, evidently, soft also. The photons with higher energies have larger absorption rate. As a result, the spectral distributions have the maximum at the boundary energy ($\varepsilon_f = 5\ MeV$ in our case) and

decrease fast while energy of created particles increases.

The kinetic equations (2) describe the cascade process in terms of the mean values giving averaged characteristics of the cascade, and do not provide any information about fluctuations in the stochastic process under consideration. An appropriate analysis constitutes much more complicate mathematical problem. These fluctuations were discussed for electromagnetic showers in amorphous media in many papers (see, e. g. [7], sect. 81). Monte-Carlo simulation procedure adequately describes all details of the cascade development but to obtain reliably averaged characteristics, sufficiently high statistics is needed. An important illustration of the scale of fluctuations is given in Fig.5 where the distribution over the multiplicity of created charged particles is shown. Let us stress out that from the solution of kinetic equations (2) we have instead of each curve in Fig.5 one number only: the mean number of created charged particles. Just these averaged characteristics are given in Figs.1-4.

Acknowledgements

We are indebted to the International Science Foundation supported in part this research by Grant N RP 6000.

References

[1] V. N. Baier, V. M. Katkov and V. M. Strakhovenko, Sov. Phys. JETP **65** (1987) 686.

[2] V. N. Baier, V. M. Katkov and V. M. Strakhovenko, Nucl. Instr. Methods **B16** (1986) 5.

[3] V. N. Baier, V. M. Katkov and V. M. Strakhovenko, Nucl. Instr. Methods **B27** (1987) 360.

[4] V. N. Baier, V. M. Katkov and V. M. Strakhovenko, Preprint BINP 95-15, Novosibirsk, 1995 Nucl. Instr. Methods (in print).

[5] R. Medenwaldt, S. P. Moller, S. Tang-Petersen et al. Phys. Lett.B **227** (1989) 483.

[6] L.D.Landau and Yu. B. Rumer Proc. Roy. Soc. **A166** (1938) 213.

[7] B.Rossi *High Energy Particles*. New York. 1952.

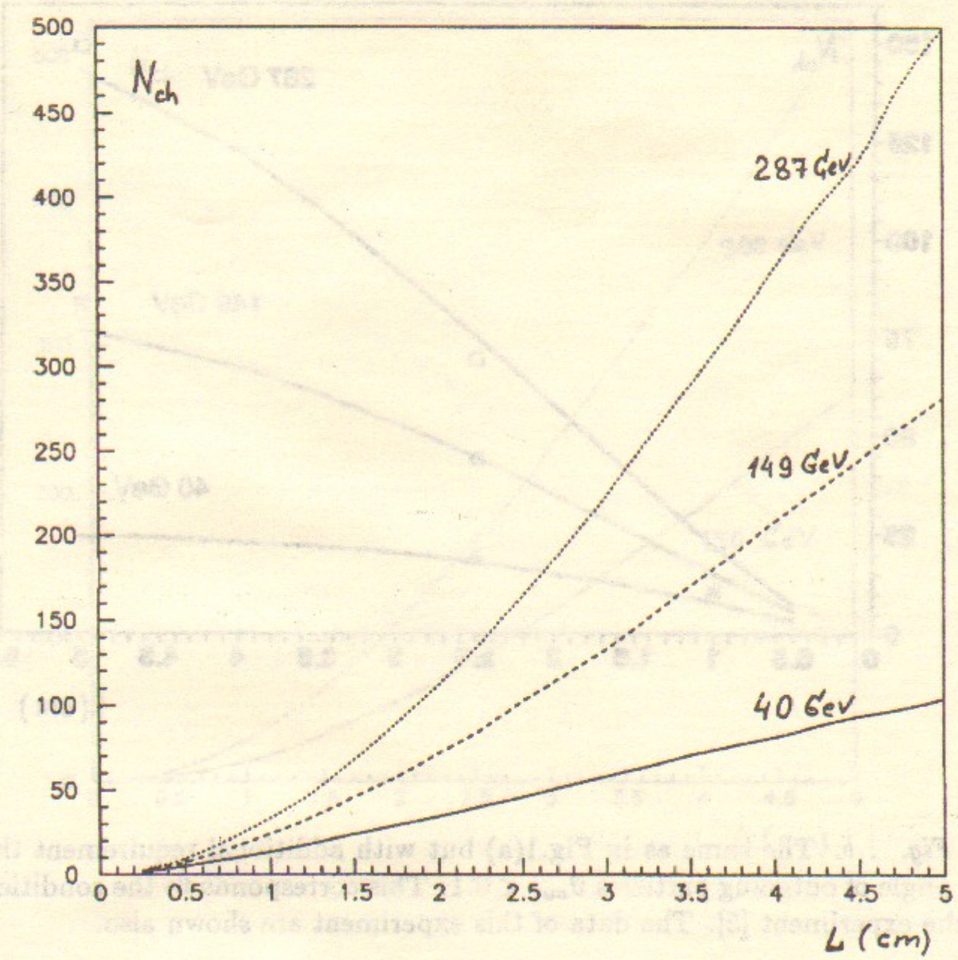

Fig. 1,a. The number of created charged particles N_{ch} with energy $\varepsilon > 5\ MeV$ vs crystal thickness. The initial particle is an electron with the energy indicated.

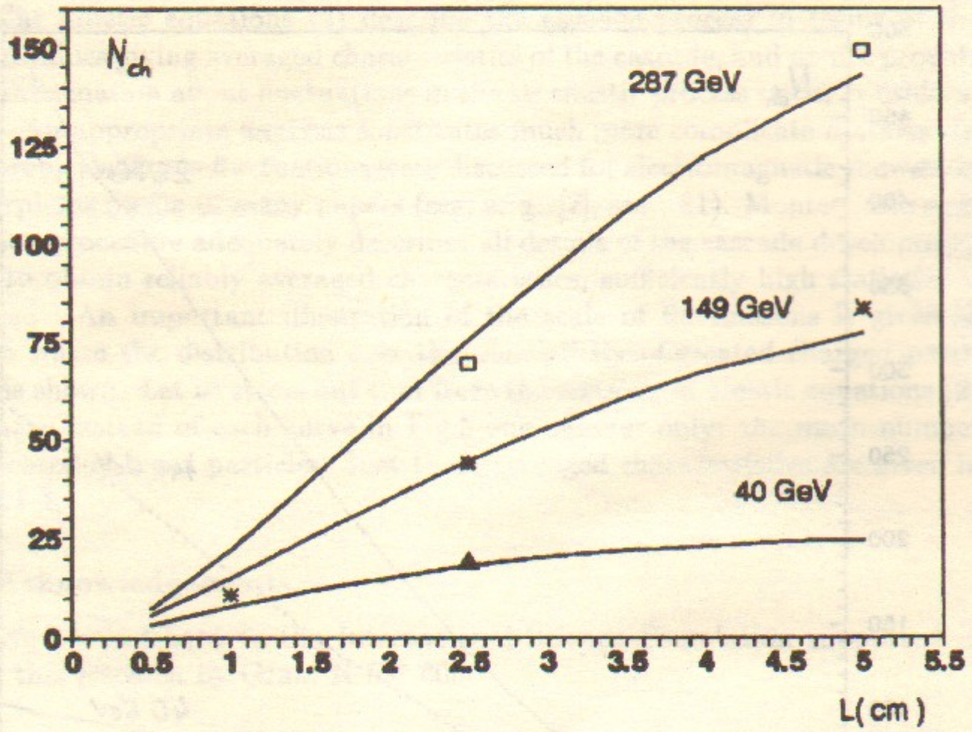

Fig. 1,b. The same as in Fig.1(a) but with additional requirement that the angle of outgoing particles $\vartheta_{out} < 0.1$. This corresponds to the conditions of the experiment [5]. The data of this experiment are shown also.

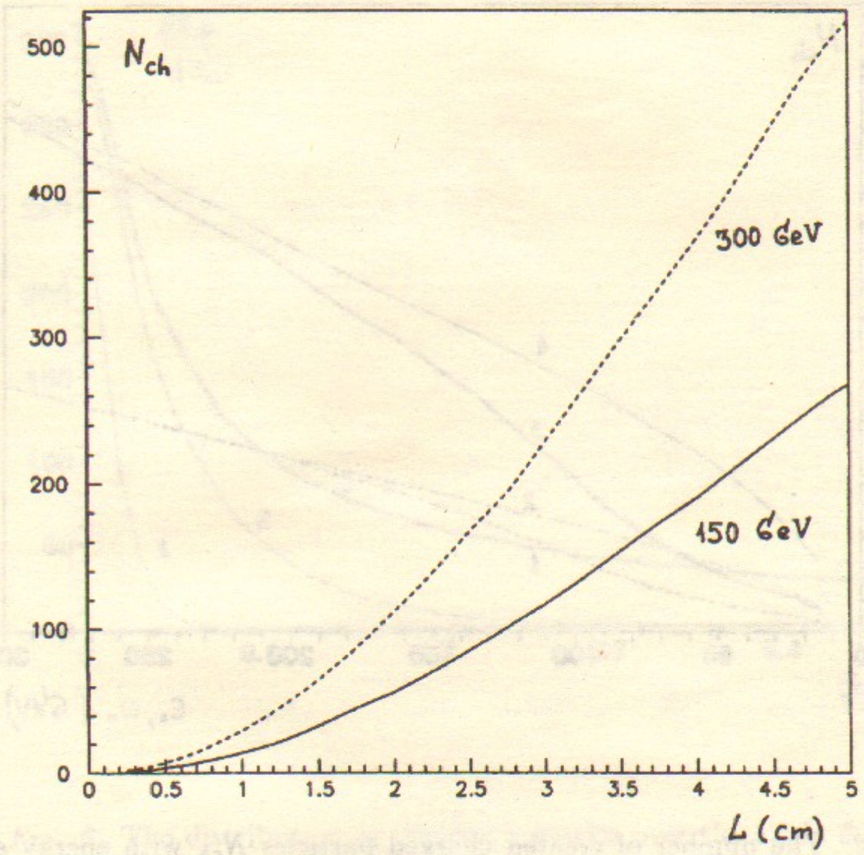

Fig. 1,c. The same as in Fig.1(a) but for initial photons with the energy indicated.

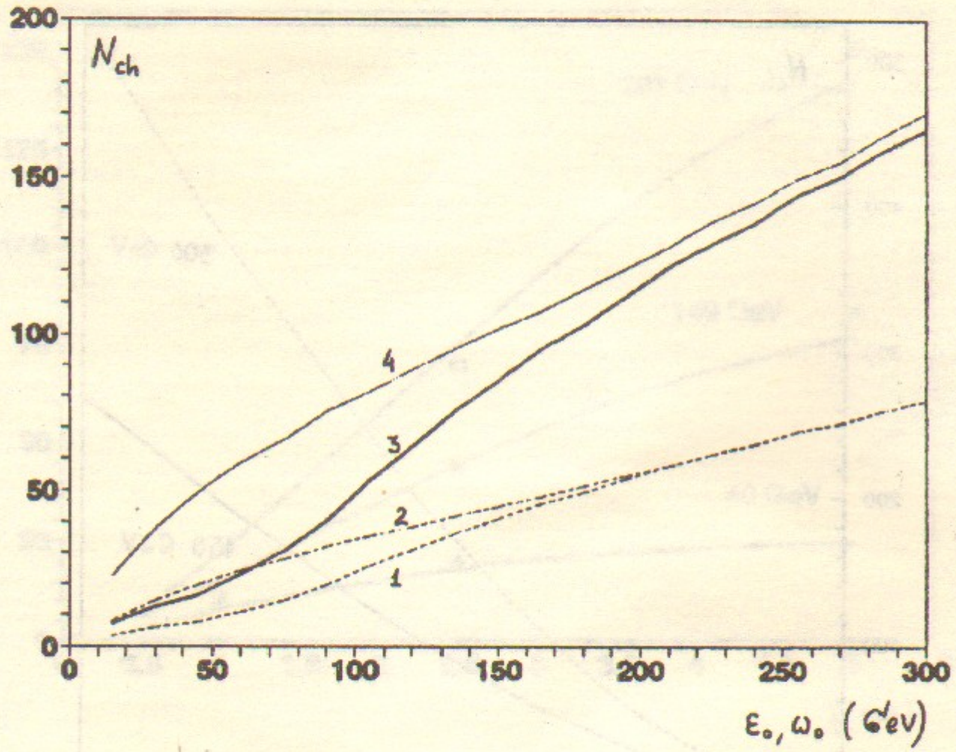

Fig. 2. The number of created charged particles N_{ch} with energy $\varepsilon > 5\ MeV$ outgoing from a crystal of thickness $L = 2.5\ cm$ vs the initial electron (curves 2 and 4) or photon (curves 1 and 3) energy with the angle $\vartheta_{out} < 0.1$ (curves 1 and 2) and with any angle ϑ_{out} (curves 3 and 4).

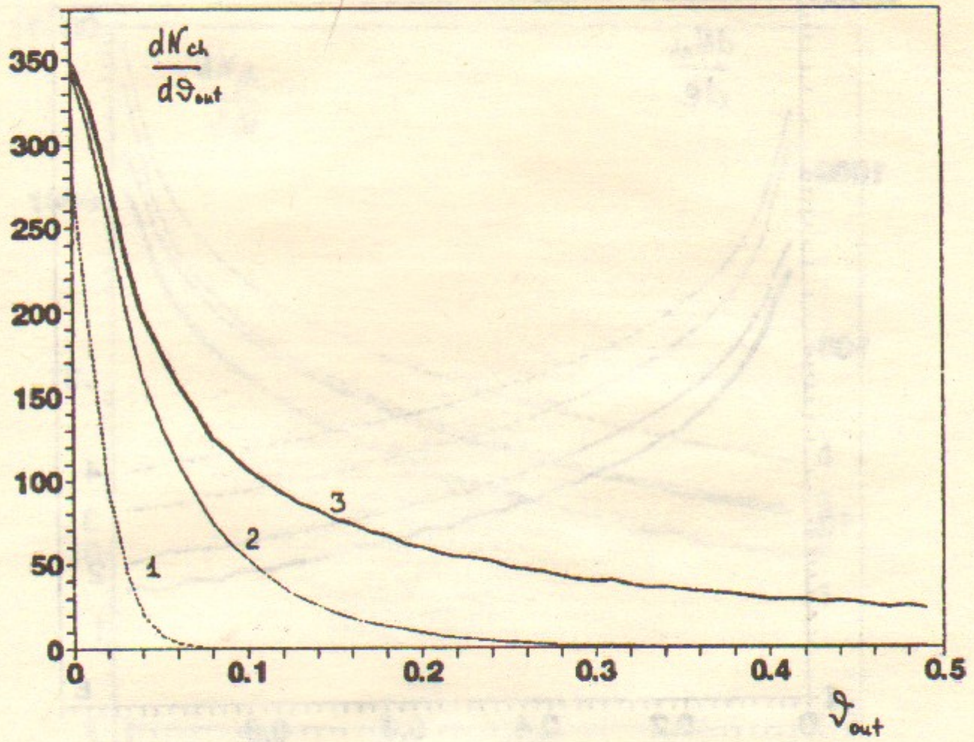

Fig. 3. The distribution of charged particles over the angle ϑ_{out} for the crystal of thickness $L = 2.5\ cm$ and the initial energy $\varepsilon_0 = 50\ GeV$. Curve 1 is for particles with energy $\varepsilon > 500\ MeV$, curve 2 is for $\varepsilon > 100\ MeV$, curve 3 is for $\varepsilon > 5\ MeV$.

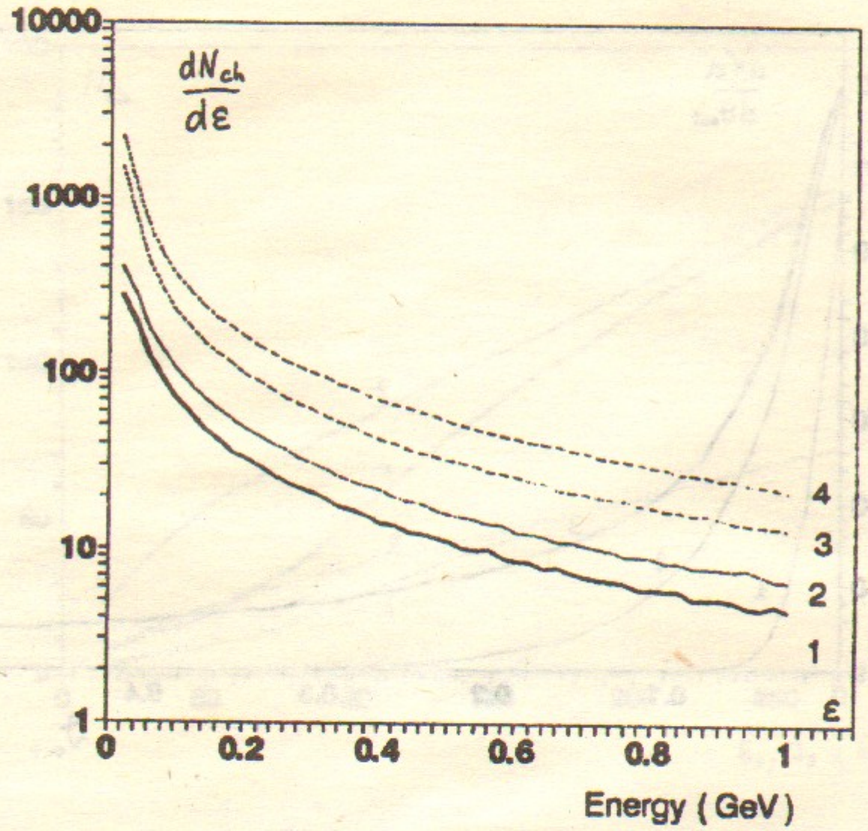

Fig. 4,a. The distribution over energy ε of charged particles for the crystal thickness $L = 1.25\ cm$ (curves 1 and 2) and for $L = 2.5\ cm$ (curves 3 and 4) at the energy of initial electrons $\varepsilon_0 = 150\ GeV$ (curves 1 and 3) and $\varepsilon_0 = 300\ GeV$ (curves 2 and 4).

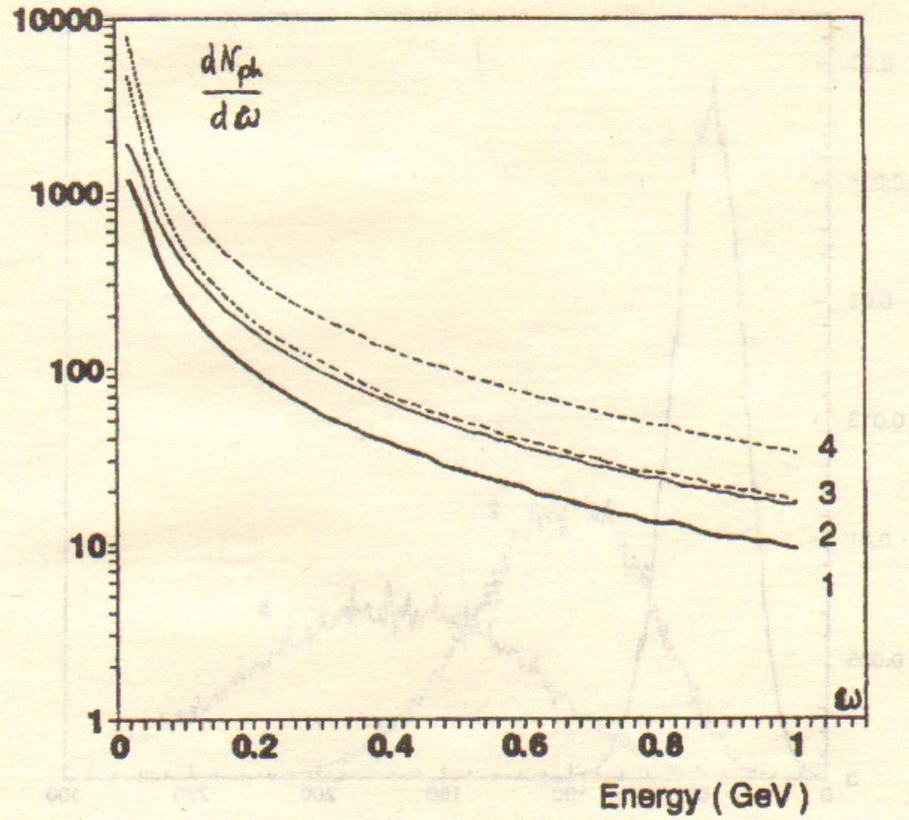

Fig.4, b. The same as in Fig.4(a) but for the distribution of photons over energy ω.

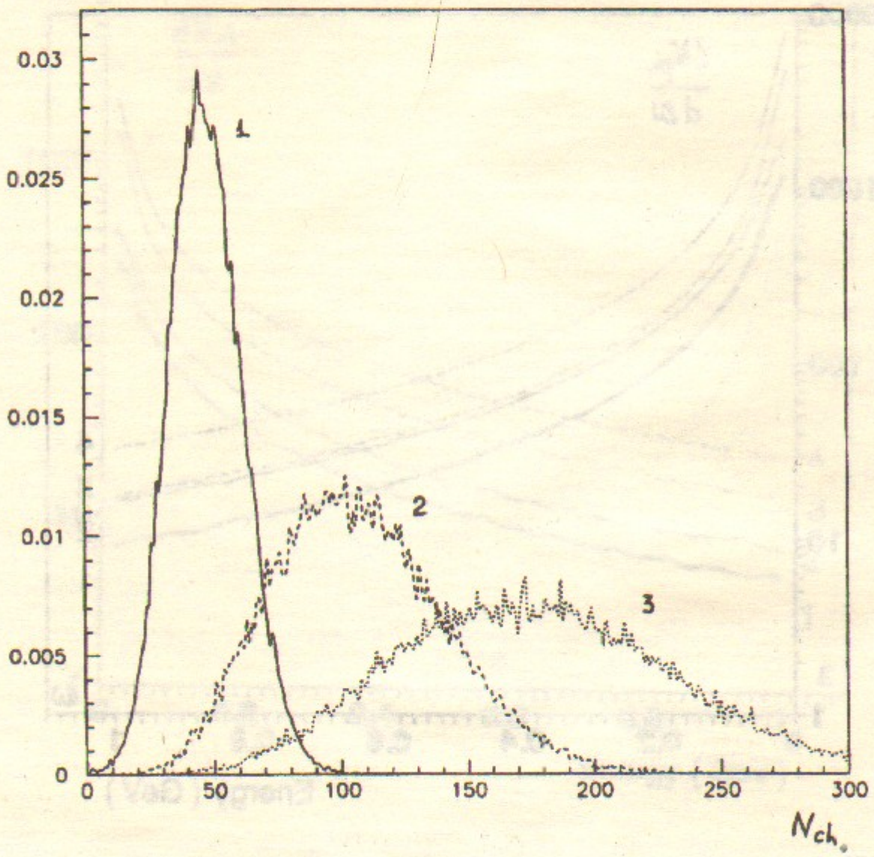

Fig.5. The distribution over the number of charged particles created in the crystal of thickness $L = 2.5\ cm$. Curve 1 is for the initial energy $\varepsilon_0 = 40\ GeV$, curve 2 is for $\varepsilon_0 = 149\ GeV$ and curve 3 is for $\varepsilon_0 = 287\ GeV$.